Journal of Materials Science and Surface Engineering, 9(1): 1071-1077
ISSN (Online): 2348-8956; DOI: https://doi.org/10.52687/2348-8956/916

Peer Reviewed

NiO-FeS_2 Heterostructure Composite: Benign Photocatalyst for Reduction of Nitrophenol to Aminophenol

Allu Ganga Raju[1] · Gandham Himabindu[1] · Yagati Vamsi Kumar[2]

[1]Department of Engineering Chemistry, AU College of Engineering, Andhra University, Visakhapatnam 530003, India.
[2]Department of Chemistry, Govt. Degree College (Men), Srikakulam 532001, India.

ABSTRACT
Aromatic nitro compounds have been promising industrial applications including paper production, pigments, pharmaceuticals, dyes, wood, leather, petrochemical, pesticides, insecticides, fungicides, explosives, and preservatives. US EPA (Environmental Protection Agency) declared that 4-nitrophenol (4-NP) has been recognized as a non-biodegradable pollutant and therefore, a very important to develop an effective method to either modify or remove 4-NP before releasing it into the environment. In that concern, we have developed an efficient, heterostructure composite of NiO-FeS_2 *via* hydrothermal. The 4 mg catalyst dose and 10 mg/L concentration of 4-NP are the optimum conditions for complete reduction of 4-NP to 4-AP by prepared NiO-FeS_2 composite.

ARTICLE HISTORY
Received 20-05-2022
Revised 13-06-2022
Accepted 16-06-2022
Published 08-09-2022

KEYWORDS
NiO-FeS_2
Hydrothermal
Reduction of 4-NP
Aminophenol.

Introduction

Aromatic nitro compounds have been promising industrial applications including paper production, pigments, pharmaceuticals, dyes, wood, leather, petrochemical, pesticides, insecticides, fungicides, explosives, and preservatives [1]. US EPA (Environmental Protection Agency) declared that 4-nitrophenol (4-NP) has been recognized as a non-biodegradable pollutant owing to its great solubility and stability in water media, also accumulated on the surface of the soil with no degradation [2]. 4-NP is carcinogenic and affects the CNS (central nervous system) that resulting in hormone imbalance and finally leading to kidney malfunctioning, eyes irritation and liver disordering [3]. Therefore, it is very important to develop an effective method to either modify or remove 4-NP before releasing it into the environment. As of now, copious purification techniques such as UV irradiation, electrocatalysis, advanced oxidation processes (AOPs), microbial degradation, have been reported for treating contaminated water [4-5], yet they have owned their disadvantages like cost with more advanced or sophisticated instruments, more time consuming and offers no better results. However, conversion of 4-NP to 4-AP (4-aminophenol) proves satisfactory results compared to removal of 4-NP from water and this reduction is greatly important from both industrial and environmental interests. Aminophenol derivatives are the intermediates for the production of many important compounds like rubber, dyestuffs and drugs. The reducing agents like sodium borohydride ($NaBH_4$) or lithium aluminium hydride ($LiAlH_4$) could be possible this reduction of 4-NP to 4-AP, but the reducing agents are unsafe to the environment and also complete reduction is not achieved by $NaBH_4$ but could be possible with nanomaterials in presence of $NaBH_4$ [1-2].

Over the past years, nanomaterials have evolved and found many applications in various fields such as pharmaceutical, medicine, engineering, textile industry, agriculture and technology among all but has only lately been studied for pollution management [6]. Because, the nanoparticles have been lauded for their splendid features with maximum adsorption opacity, strong biocompatibility and chemical inertness [7]. Among nanoparticles, nickel oxide (NiO) is a semiconductor metal oxide that has attracted particular attention in degradation of dyes or removal of pathogens from polluted water as it contains strong chemical stability and greater catalytic activity [8]. NiO has widely used in many industrial applications include capacitors, semiconductors, tuned circuits, thermistors, transparent heat mirrors, sensing devices and micro-supecapacitors [9]. Semiconductor nanoparticles are applied to other materials to strengthen their physical properties which lead to extra catalytic performance. In that sense, iron sulfide (FeS_2) is a promising material for composites making, also has great visible light response as its lower bandgap 0.95 to 1.03 eV with high light absorption coefficient (6 x 10^{-5} cm^{-1}) and is naturally occurred, stable physicochemical properties, non-toxic, and cost-effective [10-11].

Several catalysts such as Au, Cu, Ag, CuO@C dots, bimetallic Au_xAg_{1-x}, Cu nanowires, Ag@GO were reported for the reduction of 4-NP to 4-AP [11-13]. But, few of them are expensive and absent of high reduction rate. The development of innovative methods for the effective removal of toxic organic pollutants from wastewater is of paramount importance. Removal of organic pollutants from aqueous media by chemical reduction using low cost metal-based nanocatalysts and in the presence of $NaBH_4$ has become a very valuable approach in recent years. Herein, we report the cost-effective and moreover high potential composite for reduction of 4-NP to 4-AP in the presence of $NaBH_4$.

Experimental

Materials

Corresponding Author: G Himabindu, Tel: +91 9866706605
Email: himabinduauce@gmail.com
Contents lists available at http://www.jmsse.in/ & http://www.jmsse.org/

Ferric chloride ($FeCl_3$), ammonium sulphate ($(NH_4)_2SO_4$), sodium hydroxide (NaOH), copper acetate ($Cu(CH_3COO)_2$), 4-nitrophenol and sodium borohydride ($NaBH_4$) were procured from Sigma Aldrich Company, India and used without further purification. Milli Q water was used in preparing desirable solutions.

Fabrication of NiO-FeS_2 composite

Desirable composite was achieved in hydrothermal approach. In that sense, the equal amount of $FeCl_3$ (0.01M) and $(NH_4)_2SO_4$ (0.05M) were taken and mixed vigorously in a beaker for 1h. In other beaker, $Ni(NO_3)_2$ (0.01M) and NaOH (1M) solutions were mixed for 1h and added this mixer solution to first beaker and a pinch of $NaBH_4$ added. The mixed solution is transferred into Teflon lined stainless steel beaker and sealed immediately that was placed in furnace at 200 °C for 12h. After completion of reaction, the mixture solution was cooled to attain room temperature and then washed with ethanol followed by water. Finally, the obtained product was filtered and dried at 70 °C overnight in hot air stabilizer. In absence of NiO, the FeS_2 nanoparticles were synthesized by following the same procedure.

Bare NiO nanoparticles were prepared by hydrothermal route. In brief, equal volume of $Ni(NO_3)_2$ (0.01M) and NaOH (1M) aqueous solutions were taken in a beaker and mixed for 1h. $NaBH_4$ was added to above solution and transferred into a Teflon lined stainless steel beaker with immediate sealing which lies in muffle furnace at 200 °C for 3h. After completion of reaction, the mixture was cooled up to room temperature and then washed with ethanol followed by water. Finally, the obtained product was filtered and dried at 70 °C in an oven overnight.

Characterization techniques

Crystallinity of the compound was studied using XRD patterns using Bruker AXS D8 Advance X-ray diffractometer with Cu-kα wavelength at the scan rate speed of 0.02°/C. The functional groups on the catalyst surface were determined using FTIR analysis (IR prestige 21, Shimadzu) in the range from 500 to 4000 cm^{-1}. XPS (PHI 5000 versaprobe III) and UV-visible spectrophotometer (Shimadzu 2600R) used to study the optical properties of prepared samples in the wavelength of 200 to 800 nm. Morphology of prepared samples was executed by SEM (JEOL JSM-6610LV), and TEM (FEI TECNAI G2 S-TWIN).

Reduction of 4-nitrophenol experiment

The reduction of 4-nitrophenol in presence of $NaBH_4$ using prepared composite was selected as a model reaction in this study [4]. In brief, freshly prepared $NaBH_4$ aqueous solution (2.7 ml, 1 M) and 4-nitrophenol aqueous solutions (1 ml, 7x 10^{-4}) were taken in a quartz cuvette. The adequate amount of catalyst was added to the mixture solution and scanned the spectrum at regular time intervals using UV-Vis spectrometer.

Results and Discussion

The desirable NiO-FeS_2 composite was achieved through hydrothermal route, free from addition of surfactants, stabilizers, functional materials and polymers. Few researchers have been reported schematically about the formation of composites which helps to draw the formation of desirable composite as shown in Fig.1. So herein, NaOH was taken as base that controls the growth of synthesized particles. However, the reaction parameters including precursor concentration, time, temperature and solvents can influence the morphology of prepared materials.

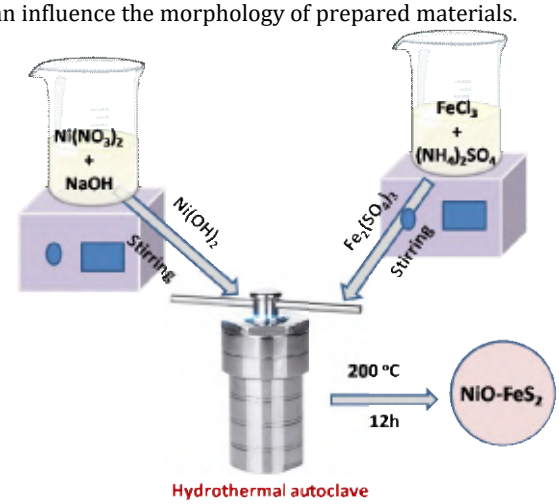

Figure 1: formation of desirable NiO-FeS_2 composite

XRD analysis is performed in this study for determine the pure phase and crystallinity of the prepared composite and blend samples. Fig.2 shows the XRD patterns of prepared blend NiO, FeS_2 and NiO-FeS_2 composite. The XRD of FeS_2 shows the patterns of 17°, 25°, 29°, 35°, 39°, 46°, 50° and 60° were concurred with previous reports and confirmed that prepared sample is pyrite [14]. NiO possess the XRD peaks at 37.6°, 43.7°, 63.2°, 75.6° and 79.5° assigned to the respective planes of (111), (200), (220), (311) and (222), concurred with cubic NiO from standard JCPDS (78-0643) [9]. NiO-FeS_2 composite exhibited the same peaks of both samples NiO and FeS_2 signify that desirable composite is made up of both individual samples without any impurities.

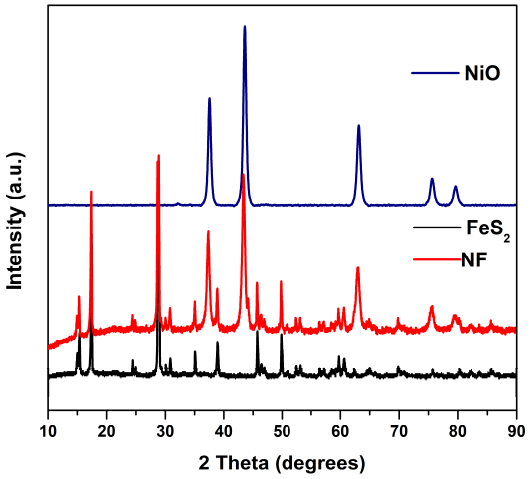

Figure 2: XRD patterns of prepared samples

From the XRD patterns, the average crystalline size (S) of prepared materials was measured using Debey Scherer's equation (1).

$$S = k\lambda / \beta \cos\theta \qquad (1)$$

Where 'λ' means the X-radiation wavelength, 'k' represents the Scherer's constant (0.94), 'β' is the full width at half maximum (FWHM) and 'θ' denotes the diffraction angle. The analysis results were found that size of prepared composite is slightly higher (Table 1) than prepared FeS_2 and NiO due to complexity of material. The prepared

composite resulting in great surface area which led to accommodate more particles on its surface.

Table 1: Crystalline size and Bandgap energy of prepared blends with their composite

Sample name	Crystalline size (nm)	*d*-spacing (A°)	Bandgap energy (eV)
FeS_2	28.6	3.08	1.68
NiO	13.5	1.5	3.6
NiO- FeS_2	21.6	2.03	2.88

The functional groups and active sites on the surface of hydrothermally prepared materials were carried out using FTIR analysis. The characteristic peak was noticed at 521 cm^{-1} for the existence of S-S stretching as well as other peak at 636 cm^{-1} attributed for the SO_4^{2-} groups as it from precursor [15]. A broad peak was located at 3416 cm^{-1} ascribed to the O-H stretching and 1642 cm^{-1} for the same stretching. A sharp identified peak at 1430 cm^{-1} due to presence of C=C group and similarly 1180 cm^{-1} for existence of C=O groups as presented in Fig.3 [16].

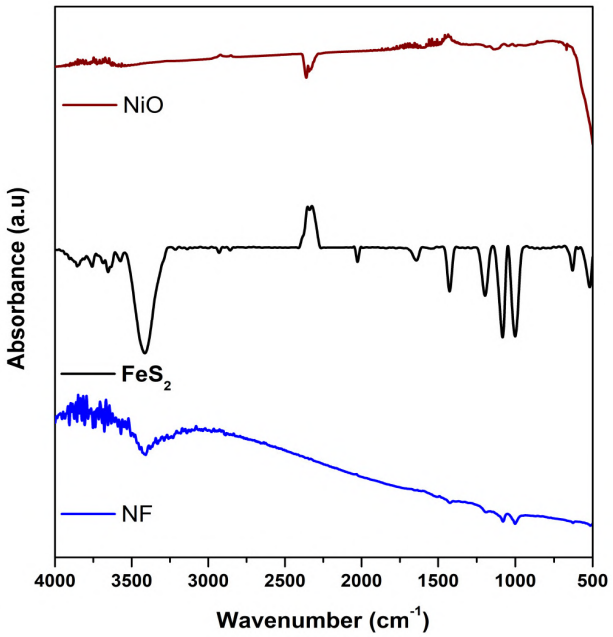

Figure 3: FTIR spectra of prepared samples

Size and shape of hydrothermally synthesized materials were carried out using electron microscopic techniques such as SEM and TEM. Fig.4 displays the SEM images of prepared composite with spherical shape and uniformity. Also noticed from the same depicts that great agglomeration due to composite formation. The surface of prepared composite was mostly smooth with a few aggregations as shown in depict with the diameter range from 100 nm to 1µm. The blend FeS_2 samples show the octahedral shape with clear structure and NiO exhibits spherical shape.

In supporting with SEM results of prepared composite for high agglomeration, TEM analysis is studied for the same. Fig.5 shows the analysis results found that nanoparticles are greatly agglomerated with almost spherical shape. The average particle size of prepared composite was measured in this study using imageJ software and found that 48 nm which is higher compared to XRD results. This is owing to the multiple crystallinity of composite. SAED analysis has a key role in confirming the high crystallinity of samples and the bright circular patterns can be seen in Fig.6c confirmed the formation of desirable composite with high purity.

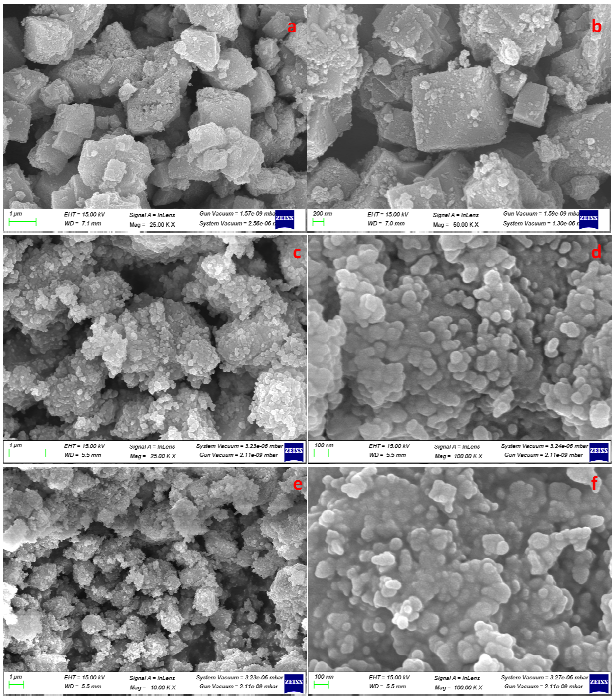

Figure 4: SEM images of prepared (a,b) FeS_2, (c,d) NiO and (e,f) NiO-FeS_2 composite

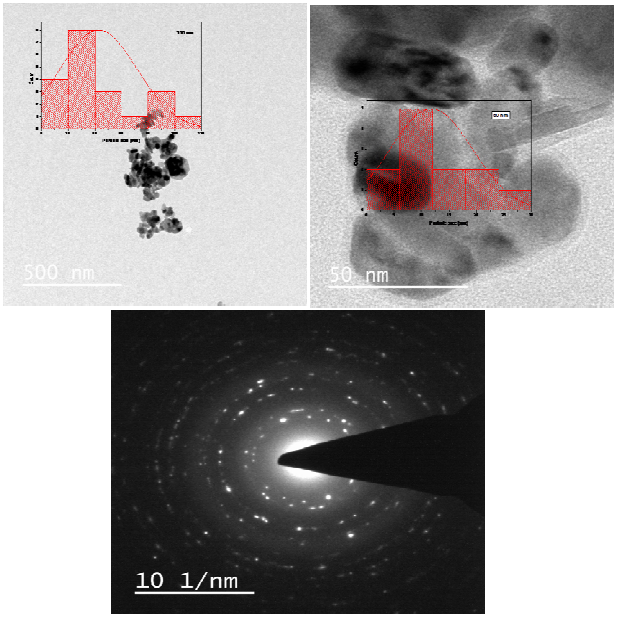

Figure 5: TEM with respective histogram distribution images and SAED graph of prepared NiO-FeS_2

Energy dispersive x-ray spectroscopy (EDX) analysis was performed in this study to identify the elements consistency in prepared samples. Fig.6 shows the EDX spectrum of hydrothermally prepared composite that contains desirable elements such as iron (Fe), nickel (Ni), oxygen (O) and sulphur (S) means the purest form of NiO-FeS_2 composite is formed without any impurities.

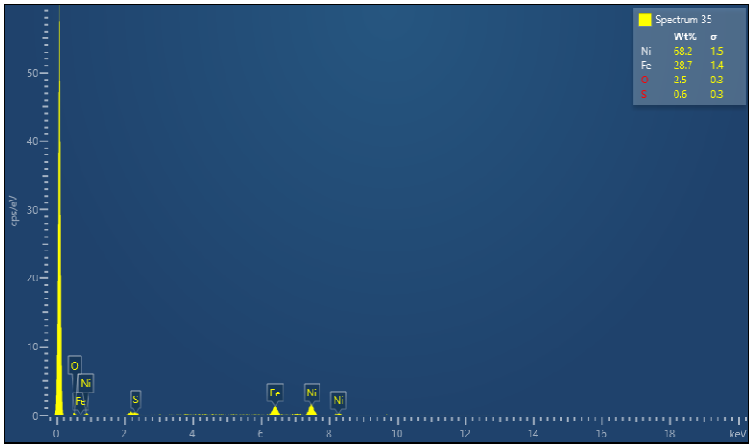

Figure 6: EDX spectrum of prepared NiO-FeS_2 composite

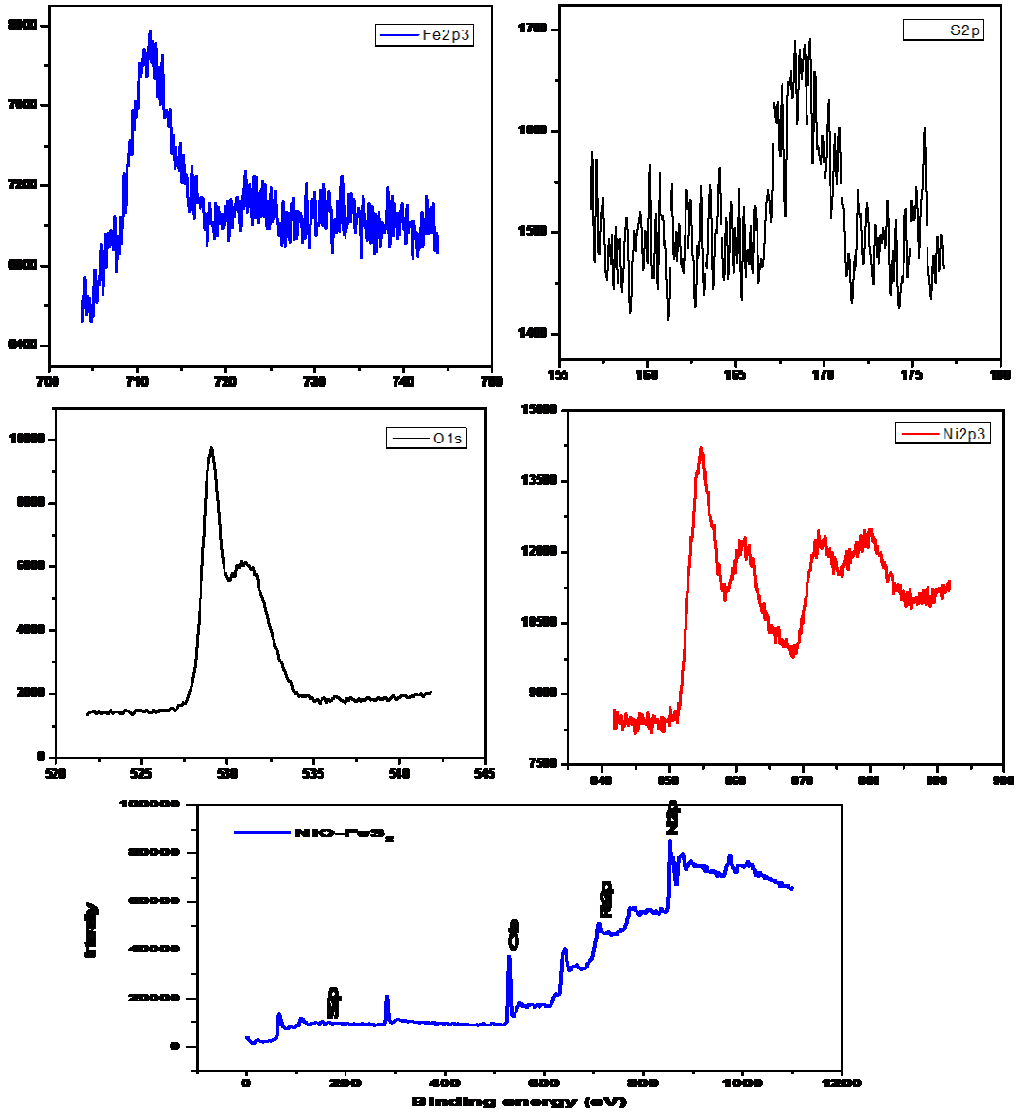

Figure 7: XPS analysis result of prepared NiO-FeS_2 composite with elements consistency

In supporting with EDX analysis for the identification of elemental consistency of prepared composite, XPS analysis is executed in this study. However, the desirable composite is formed with elements such as Fe, S, Zn and O as shown in Fig.7. Ni 2p3/2 spectrum has two peaks are located at 854.6 and 861.2 eV which accounted for Ni^{2+} ions [17]. The high-resolution peak was noticed at 530 eV was assigned to the existence of O [18]. The Fe 2p spectra of prepared NF composite is dominated by a pyrite peak at 711 eV implies the Fe exist in Fe 2p 3/2 [19] which is much closer to literature (707.3 eV). The S spectrum shows a peak at 169 eV signifies that disulfide is formed and owing to the sulphates (SO_4^{2-}) is believed to be formed by the exposure of the pyrite product to air [20].

Contents lists available at http://www.jmsse.in/ & http://www.jmsse.org/

UV DRS analysis

The extraordinary performance of photocatalyst decided by the major factor is bandgap energy of material, if it is small that possess higher degradation rate. Hence, we have studied the bandgap energy of prepared materials using established Tauc plot equation as Eq 2.

$$\alpha h\upsilon = A\,[h\upsilon - Eg]n/2 \qquad (2)$$

Where 'α' is the absorption coefficient, 'A' is the constant and 'n' indices indirect (n = ½) or direct (n = 2) bandgap material. Also 'E_g' is bandgap energy, 'λ' is wavelength corresponds to the absorption edge. The results of bandgap were found to be 3.6, 1.68 and 2.88 eV for NiO, FeS_2 and NiO-FeS_2 composite respectively. The insertion of FeS_2 to NiO results decreases the bandgap of NiO as shown in Fig.8. Hence, it can accommodate more species on its surface and this composite could be more promising adsorbent.

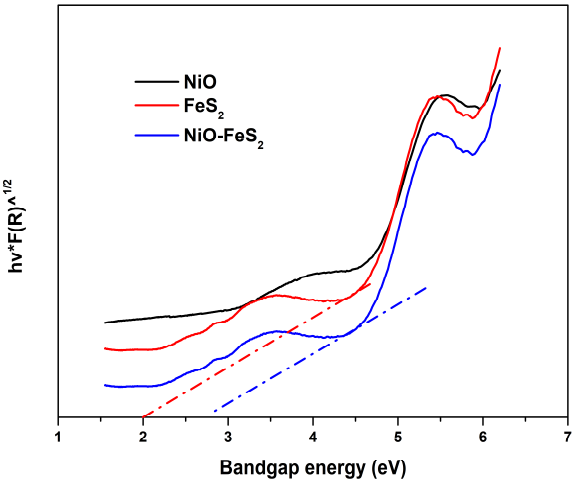

Figure 8: DRS spectral analysis of prepared samples

Reduction of 4-NP to 4-AP

The reduction of 4-NP is commonly employed model reaction used to determine the catalytic activity of prepared composite. Since 150 years, the nitroarene reduction has been known [11]. Then, the reaction has been shown to be catalyzed by a wide variety of materials such as metal-free powders, nanoparticulate metals, supported metals like photocatalysts. This reaction is favoured at room temperature and completely monitored by UV-Vis spectroscopy as designated in Fig.9. The reaction quantitatively monitored using UV-Visible spectrometer and the maximum absorbance (λ_{max}) of 4-NP occurred at 400 nm [7]. There is no specific change in the absorption peak shift when adding $NaBH_4$ to 4-NP and the same happens with the addition of NiO. Based on literature, the reaction does not occur in the absence of catalyst or at ambient temperature/pressure in aqueous solutions. Hence, the composite was added to the tested mixture solution and the absorbance was decreased successfully and the evolution of a peak formed at 298 nm which quantify the 4-aminophenol (4-AP). This signifies the reduction of 4-NP to 4-AP in presence of $NaBH_4$ using prepared composite (Fig.10). The colour of initial solution turned into yellow (usually 4-nitrophenolate ion) after addition of $NaBH_4$ to 4-NP is evident from the bathochromic shift (from 298 nm to 400nm) owing to the 4- NP possesses auxochromic nature. In general $NaBH_4$ favours the reduction process of 4-NP but could not process as large difference in potential among donor BH_4^- and acceptor 4-NP. However, the entire reduction process was monitored by UV-Vis spectroscopy at regular time intervals and found that the intensity of absorption peak at 400 nm was deceased with time increments, simultaneously a new peak was formed at 298 nm which accounts for the presence of 4-AP.

The experimental conditions were optimized with respect to catalyst dose and 4-NP concentration. The effect of catalyst amount was studied by using 5, 4, and 3mg, the analysis results found that 4mg composite showed high reduction rate of 4-NP (98%) in 60 min (Fig.11a) and 3 mg catalyst reduces 4-NP with 86%. The initial concentration of 4-NP also monitored with 10, 15 and 20 mg/L, the results figured out 10 mg/L of 4-NP was almost converted into 4-AP in 1h and there is no remarkable reduction after 20 mg/L (Fig.11b). Other concentrations of 4-NP like 15 mg/L showed 91% and 20 mg/L exhibited 82% reduction rate. The 4 mg catalyst dose and 10 mg/L concentration of 4-NP are the optimum for complete reduction of 4-NP to 4-AP by prepared composite NiO-FeS_2.

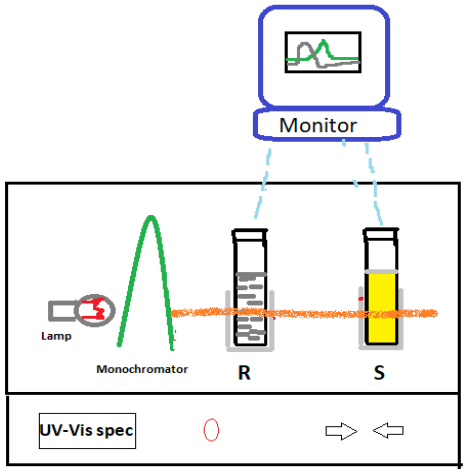

Figure 9: Illustration of UV-Vis spectral analysis on reduction of 4-NP

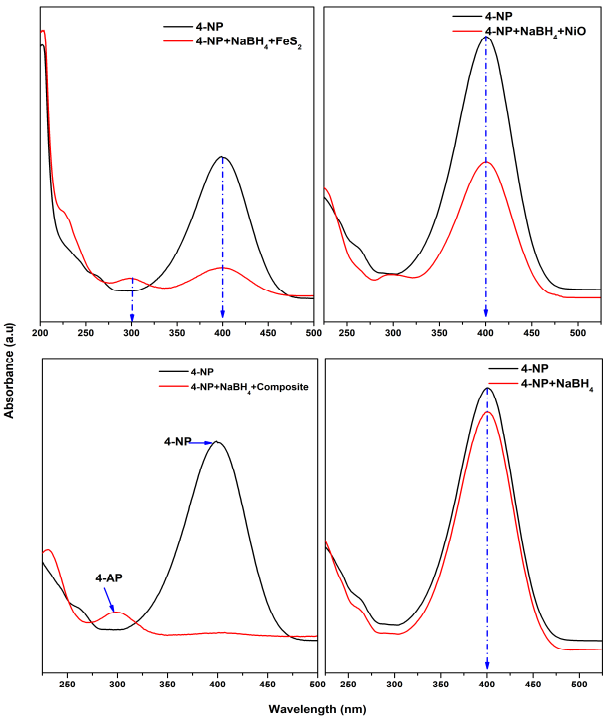

Figure 10: Reduction of 4-NP to 4-AP using prepared samples

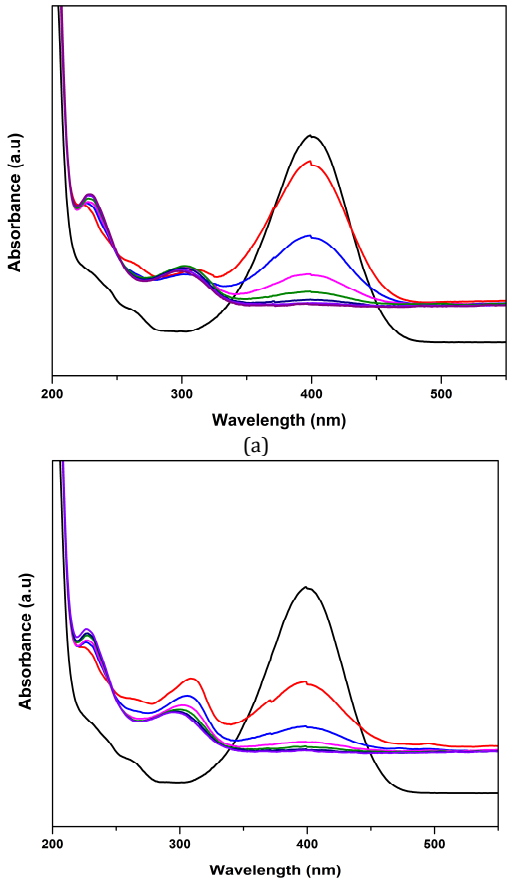

Figure 11: Reduction of 4-NP at (a) 4mg catalyst dose and (b) 10 mg/L 4-NP aqueous solution

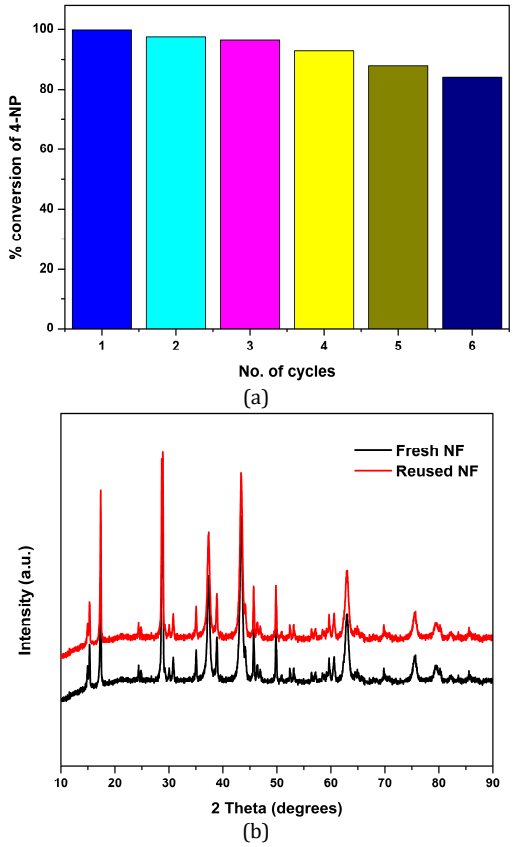

Figure 12: (a) Reusability of prepared NiO-FeS_2 composite (b): Stability of prepared NiO-FeS_2 composite after reusability

Stability and recycling

The prepared composite was further examined for its recyclability and stability towards the reduction of 4-nitrophenol. In view of that, after reduction experiment, the used composite was collected through centrifugation frequently and filtered the same. The water and ethanol used for cleaning the used composite and the same utilised for the fresh reduction experiment. Interestingly, the used composite showed greater reduction performance and the same composite used for further fresh experiments. The reduction rate was tremendously decreased up to 84% with experiments raised till six as shown in Fig.12a due to weight loss of composite during collection or washing of it. Significant remark is noticed from the XRD analysis that the patterns are same for recycled composite as in fresh (Fig.12b). The analysis results stated that the prepared composite can be recycled and stable for reduction of 4-nitrophenol.

Conclusions

4-Nitrophenol Aromatic nitro compounds have great applications in industries of dyes, pigments, pesticides and pharmaceutical. These compounds cause severe damage to environment, animals, humans and plants. 4-Nitrophenol has received a great attention in this sense and US EPA declared that 4-NP is a major pollutant and not degraded significantly. Nanomaterials have proven the best alternative for removal of pollutants. Therefore, we have examined the reduction of 4-NP using nanocomposite i.e. NiO-FeS_2. Hydrothermal method was employed in this study for achieved the desirable composite. The sophisticated instruments were used in this study to characterize the samples for their optical, electronic and structural properties. NiO-FeS_2 composite exhibits spherical shape with uniformity and also noticed that great agglomeration due to composite formation. The results of bandgap were found to be 3.6, 1.68 and 2.88 eV for NiO, FeS_2 and NiO-FeS_2 composite respectively. The reduction of 4-NP to 4-AP using prepared composite in presence of $NaBH_4$ was examined and the colour of initial solution turned into yellow (usually 4-nitrophenolate ion) after addition of $NaBH_4$ to 4-NP is evident from the bathochromic shift (from 298 nm to 400nm) owing to the 4- NP possesses auxochromic nature. The 4 mg catalyst dose and 10 mg/L concentration of 4-NP are the optimum conditions for complete reduction of 4-NP to 4-AP by prepared NiO-FeS_2 composite.

Acknowledgement

The author A Ganga Raju expresses his sincere thanks to the principal of MR College (A), Vizianagaram for their great support and also extends his gratitude to Bio Enviro Chemical Solutions (BECS), Visakhapatnam for providing the best characterisation analysis results.

Conflicts of interest

Authors stated that there are no conflicts of interest.

References

1. AA Kassema, HN Abdelhamid, DM Fouada, SA Ibrahim, Catalytic reduction of 4-nitrophenol using copper terephthalate frameworks and CuO@C composite, J Envi Chem Engg., 2021, 9(1), 104401.
2. Ravi, M Sarasija, D Ayodhya , LS Kumari, D Ashok, Facile synthesis, characterization and enhanced catalytic reduction of 4-nitrophenol using NaBH4 by undoped and Sm3+, Gd3+,

Hf3+ doped La2O3 nanoparticles, Nano Convergence, 2019, 6, 12.
3. AS Hashimi , MANM Nohan, SX Chin, S Zakaria, CH Chia, Rapid Catalytic Reduction of 4-Nitrophenol and Clock Reaction of Methylene Blue using Copper Nanowires, Nanomaterials 2019, 9, 936.
4. SM Botsa, YP Kumar, K Basavaiah, Facile simultaneous synthesis of tetraaniline nanostructures/silver nanoparticles as heterogeneous catalyst for the efficient catalytic reduction of 4-nitrophenol to 4-aminophenol, RSC Adv., 2020, 10 (37), 22043-22053.
5. G Ravi, M Sarasija, D Ayodhya , LS Kumari, D Ashok, Facile synthesis, characterization and enhanced catalytic reduction of 4-nitrophenol using NaBH4 by undoped and Sm3+, Gd3+, Hf3+ doped La2O3 nanoparticles, Nano Convergence, 2019, 6, 12.
6. SM Botsa, K Basavaiah, Fabrication of multifunctional TANI/Cu2O/Ag nanocomposite for environmental abatement, Sci Rep., 2020, 10, 1-16.
7. P Hervés, MP Lorenzo, LLM Marzán, J Dzubiella, Y Lu, M Ballauff, Chem. Catalysis by metallic nanoparticles in aqueous solution: model reactions, Soc. Rev. 2012, 41, 5577–5587.
8. A Akbari, Z Sabouri, HA Hosseini, A Hashemzadeh, M Khatami, M Darroudi, Effect of nickel oxide nanoparticles as a photocatalyst in dyes degradation and evaluation of effective parameters in their removal from aqueous environments, Inorganic Chemistry Communications, 115, 2020, 107867.
9. GS Sree, SM Botsa, KVB Ranjitha, BJM Reddy, Enhanced UV–Visible triggered photocatalytic degradation of Brilliant green by reduced graphene oxide based NiO and CuO ternary nanocomposite and their antimicrobial activity, Arab J Chem., 2020, 13 (4), 5137-5150.
10. Wang, N., Wang, J., Liu, M. Preparation of FeS2/TiO2 nanocomposite films and study on the performance of photoelectrochemistry cathodic protection, Sci Rep., 2021, 11, 7509.
11. J Strachan, C Barnett, AF Masters, T Maschmeyer, 4-Nitrophenol Reduction: Probing the Putative Mechanism of the Model Reaction, ACS Catal., 2020, 10, 5516−5521.
12. RD Neal, Y Inoue, RA Hughes, S Neretina, Catalytic Reduction of 4-Nitrophenol by Gold Catalysts: The Influence of Borohydride Concentration on the Induction Time, J. Phys. Chem. C 2019, 123, 12894−12901.
13. AS Hashimi, MANM Nohan, SX Chin, S Zakaria, CH Chia, Rapid Catalytic Reduction of 4-Nitrophenol and Clock Reaction of Methylene Blue using Copper Nanowires, Nanomaterials 2019, 9, 936.
14. X Min, Y Li, Y Ke, M Shi, LCK Xue, Fe-FeS2 adsorbent prepared with iron powder and pyrite by facile ball milling and its application for arsenic removal, Water Sci Tech., 2017, 76.1, 192-200.
15. E Bastola, KP Bhandari, RJ Ellingson, Application of composition controlled nickel-alloyed iron sulfide pyrite nanocrystal thin films as the hole transport layer in cadmium telluride solar cells, J.Mater.Chem.C, 2017, 5, 4996—5004.
16. GS Sree, BS Mohan, BJM Reddy, KVB Ranjitha, Deterioration of Cadmium and pathogens from contaminated water using hydrothermally prepared NiO-ZnO-RGO composite, J Mater Res Tech., 2021, 10, 976-987.
17. C Venkataramana, SM Botsa, P Shyamala, R Muralikrishna, Photocatalytic degradation of polyethylene plastics by NiAl 2 O 4 spinels-synthesis and characterization, Chemosphere, 2021, 265, 129021.
18. L. Samad, M. Cabán – Acevedo, M. J. Shearer, K. Park, R. J. Hamers, Surface and shape modification of mackinawite (FeS) nanocrystals by cysteine adsorption: A first-principles DFT-D2 study, Chem. Mater. 2015, 27, 3108-3114.
19. C. M. Eggleston, J. Ehrhardt, W. Stumm, Surface structural controls on pyrite oxidation kinetics: An XPS-UPS, STM, and modeling study, Am. Mineral. 1996, 81, 1036-1056.
20. S. Seefeld, M. Limpinsel, Y. Liu, N. Farhi, A. Weber, Y. Zhang, N. Berry, Y. J. Kwon, C. L.Perkins, J. C.Hemminger, R. Wu, M. Law, Iron pyrite thin films synthesized from an Fe(acac)3 ink, J. Am. Chem. Soc. 2013, 135, 4412-4424.